

Fermilab

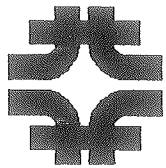
SSC DETECTOR SOLENOID DESIGN NOTE #106

TITLE: Comparison of Air Core and Iron Return Solenoid Magnetic and Structural Characteristics

AUTHOR: Bob Wands

DATE: Dec. 18, 1989





## Comparison of Air Core and Iron Return Solenoid Magnetic and Structural Characteristics

Bob Wands

### Introduction

The solenoid collaboration meeting at ANL on Nov. 16-17, 1989 selected four solenoid geometries for further study. These geometries, and the abbreviations used in this report, are:

1. FTD-A, Iron Return Solenoid,  $r=1.8$  m, central field = 2.0 T,  $l=14$  m.
2. FTD-B, Iron Return Solenoid,  $r=2.1$  m, central field = 1.8 T,  $l=14$  m.
3. ACS-A, Air Core Solenoid,  $r=1.8$  m, central field = 2.0 T,  $l=8$  m.
4. ACS-B, Air Core Solenoid,  $r=2.1$  m, central field = 1.8 T,  $l=8$  m.

The purpose of this report is to summarize the magnetic field distribution and the conductor and support cylinder radial thicknesses for these four geometries.

In addition to the four geometries above, which assumed uniform current density along the length of the solenoid, an additional geometry, called ACS-C, was analyzed which used the air core geometry ACS-A and two individual current densities to produce a more uniform field. The ACS-A and ACS-C results were used to calculate the shear stress between the conductor and support cylinder.

### Finite Element Models

The solenoids, air and iron were modeled with the ANSYS STIF13 multifield solid axisymmetric finite element. A b-h curve for 1020 steel was used. The support cylinder was modeled with STIF61 conical shell elements. The cylinder was coupled in displacement with the conductor to simulate the epoxy bond between these structures. Figs. 1 and 2 show typical meshes for the FTD and ACS models.

The model ACS-A was modified for two current densities (ACS-C) in an effort to produce a more uniform axial field. Closed form solenoid calculations (see Appendix A) were used to find two current densities (one over the innermost 6 m and another over the two outermost 1 m lengths) which produced a central field of 2 T and a field at the solenoid ends of 2 T.

## Results and Discussion

Figs. 3 and 4 show flux plots typical of the FTD and acs geometries. Table I summarizes the axial and hoop electromagnetic forces. The axial force is calculated from  $\mathbf{J} \times \mathbf{B}$  and summed over the coil; The hoop force is calculated based on the maximum hoop stress in the conductor, and is expressed as Newtons per axial length of coil.

Tables II and III summarize the following quantities for each model for 5000 A and 10000 A, respectively:

1. The total inductance, calculated by ANSYS from the magnetic solution.
2.  $t_s$ , the radial thickness of conductor stabilizer based on adiabatic quench characteristics. <sup>(1)</sup>
3.  $t_{sc}$ , the radial thickness of the support cylinder based on hoop stress requirements. The conductor stabilizer and support cylinder are assumed to be made of aluminum. The maximum conductor strain is assumed to be 0.1%, and the maximum hoop stresses for the conductor and the support cylinder are  $3670 \text{ N/cm}^2$  (5300 psi) and  $9200 \text{ N/cm}^2$  (13000 psi), respectively. <sup>(1)</sup>
4.  $L_r$ , the total radiation length of the conductor/support cylinder in the radial direction.

The tables show that for both the small diameter (1.8 m) and large diameter (2.1 m) designs, the air core solenoid design results in a thinner conductor in terms of radiation lengths through the radial direction of the conductor/support cylinder assembly. The axial forces on the ACS models are much larger than those of the FTD models, as expected.

The line integral of the cross product of the field vector with the position vector along a ray extending from the center of the solenoid to the current sheet is a measure of the phi bending power of the field for high momentum particles. This integral, called Bdl, is plotted in Figs. 5-8 as a function of

pseudorapidity (defined as  $-\ln \cdot \tan(\theta/2)$  where  $\theta$  is the angle of the ray with the longitudinal solenoid axis). The most uniform Bdl is found for the FTD models, due to their more uniform axial field. Another measure of field uniformity is the variation of the axial component of the B-field at a constant radius as a function of pseudorapidity. Figs. 9-12 show this variation.

The axial component of the B-field for ACS-C is shown in Fig. 13 and verifies that the predicted 2 T field at the center and ends was achieved, although accompanied by a large increase in field just inside the end. Fig. 14 compares the Bdl integrals for the ACS-A and ACS-C geometries, showing the considerable improvement in the Bdl for the ACS-C. The large increase in B-field near the end of the magnet is probably not practical, and future work will look at using three different current densities in an effort to reduce this effect.

The ACS-A and ACS-C geometries were used to provide conductor force input for a refined structural model of the conductor and support cylinder. The resulting shear stress distributions between the coil stabilizer and the support cylinder are shown in Figs. 15 and 16. It is clear that the two current density approach will increase shear stress, although the maximum numbers here are thought to be reasonable working stresses for the epoxy bond, and there is evidence from ongoing work that a more refined analysis will find the stresses to be considerably smaller than calculated here.

### Conclusions

The ACS models produce the thinnest radial designs, as anticipated, primarily due to their smaller length and hence smaller inductance, which produces less adiabatic heating during a quench. The large fringe field must be considered in the calorimetry design. The ACS can be built with a current density graded along its length to produce a more uniform field, although this will increase the axial forces on the conductor and the shear stress between the conductor and support cylinder.

### References

1. Wands, B., 'Stabilizer and Support Cylinder Thickness for Three SSC Solenoid Geometries Based on Adiabatic Quench and Magnetic Stress Requirements', SSC Detector Solenoid Design Note #102, November 20, 1989

Table I. Summary of Magnetic Force and Shear Stress Results

| Model | Axial Force (N)        | Hoop Force (N/cm)      |
|-------|------------------------|------------------------|
| FTD-A | 5.07(10 <sup>6</sup> ) | 2.88(10 <sup>4</sup> ) |
| FTD-B | 4.18(10 <sup>6</sup> ) | 2.42(10 <sup>4</sup> ) |
| ACS-A | 16.4(10 <sup>6</sup> ) | 2.96(10 <sup>4</sup> ) |
| ACS-B | 16.1(10 <sup>6</sup> ) | 2.53(10 <sup>4</sup> ) |

Table II. Summary of Inductance and Coil and Support Cylinder Thickness for 5000 A

| Model | Inductance (H) | $t_s$ (cm) | $t_{sc}$ (cm) | $L_r$ |
|-------|----------------|------------|---------------|-------|
| FTD-A | 18.13          | 7.40       | 0.19          | 0.84  |
| FTD-B | 17.85          | 6.05       | 0.22          | 0.70  |
| ACS-A | 10.21          | 5.94       | 0.85          | 0.75  |
| ACS-B | 10.40          | 5.22       | 0.67          | 0.65  |

Table III. Summary of Inductance and Coil and Support Cylinder Thickness for 10000 A

| Model | Inductance<br>(H) | $t_s$<br>(cm) | $t_{sc}$<br>(cm) | $L_r$ |
|-------|-------------------|---------------|------------------|-------|
| FTD-A | 4.53              | 5.04          | 1.12             | 0.68  |
| FTD-B | 4.46              | 4.16          | 0.97             | 0.57  |
| ACS-A | 2.55              | 4.04          | 1.60             | 0.63  |
| ACS-B | 2.60              | 3.58          | 1.33             | 0.54  |

ANSYS 4.4

DEC 21 1989

09:23:34

PLOT NO. 1

PREP7 ELEMENTS

TYPE NUM

ZV =1

DIST=6.16

XF =2.523

YF =-5.6

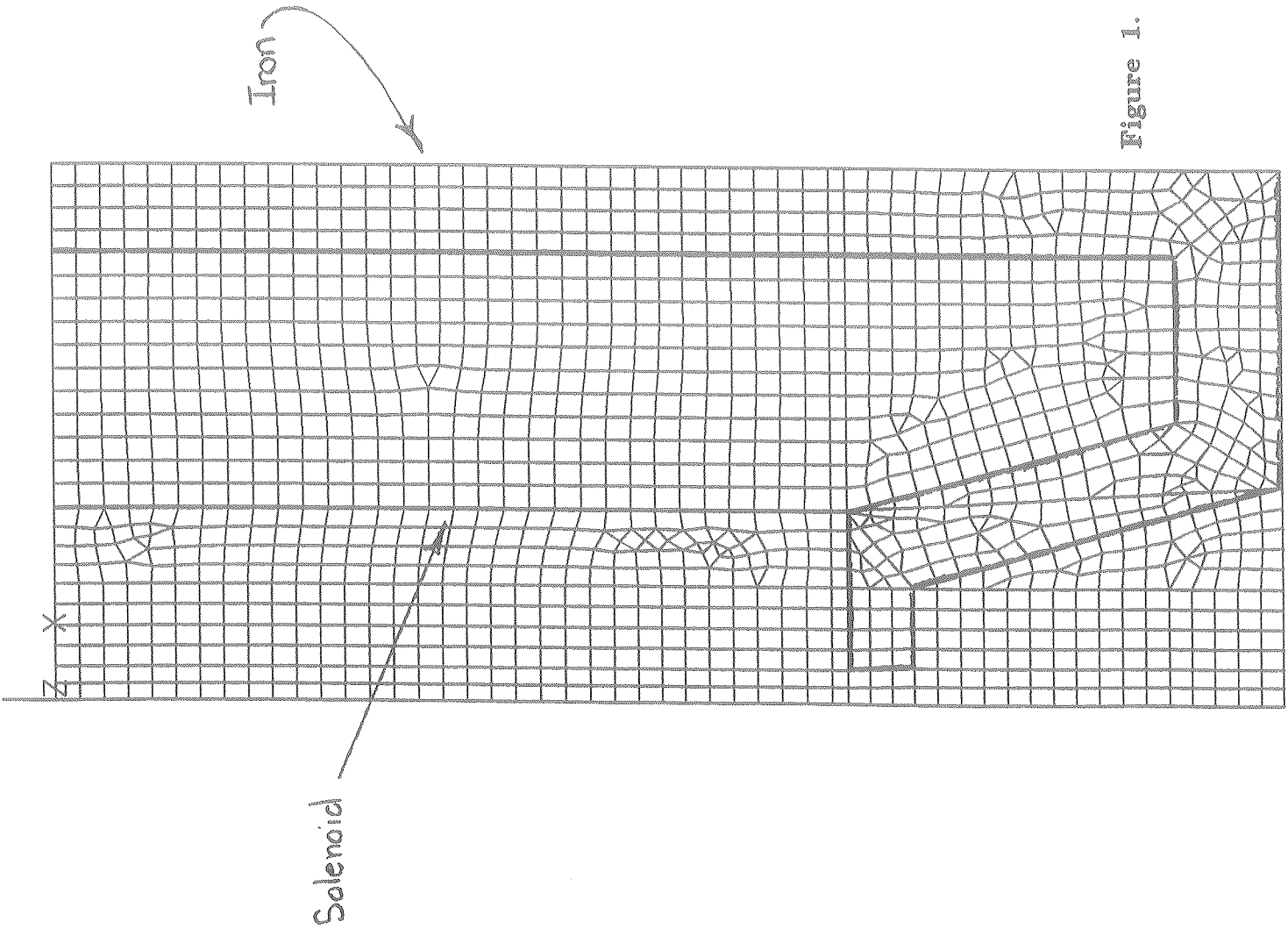


Figure 1. Finite Element Model of Iron Return Solenoid

ANSYS 4.4

DEC 21 1989

09:25:35

PLOT NO. 1

PREP7 ELEMENTS

TYPE NUM

ZV =1

DIST=4.675

XF =3

YF =-4.25

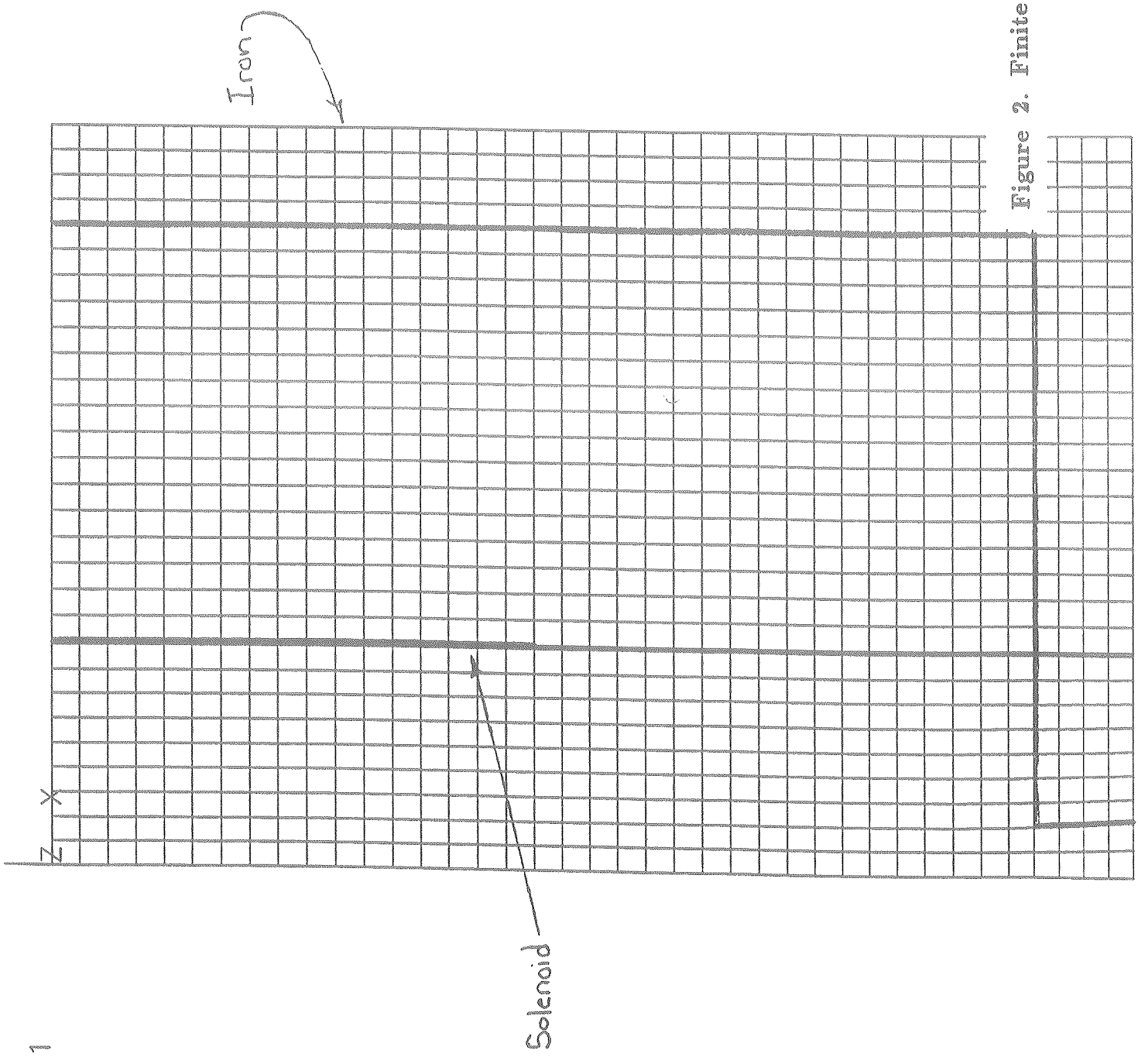


Figure 2. Finite Element Model of Air Core Solenoid

ANSYS 4.4  
DEC 15 1989  
10:05:16  
PLOT NO. 2  
POST1 STRESS  
STEP=2  
ITER=10  
MAG  
SMX =3.281

ZV =1  
DIST=6.16  
XF =2.523  
YF =-5.6  
EDGE

$\Gamma = 1.8 \times 10^{-7}$

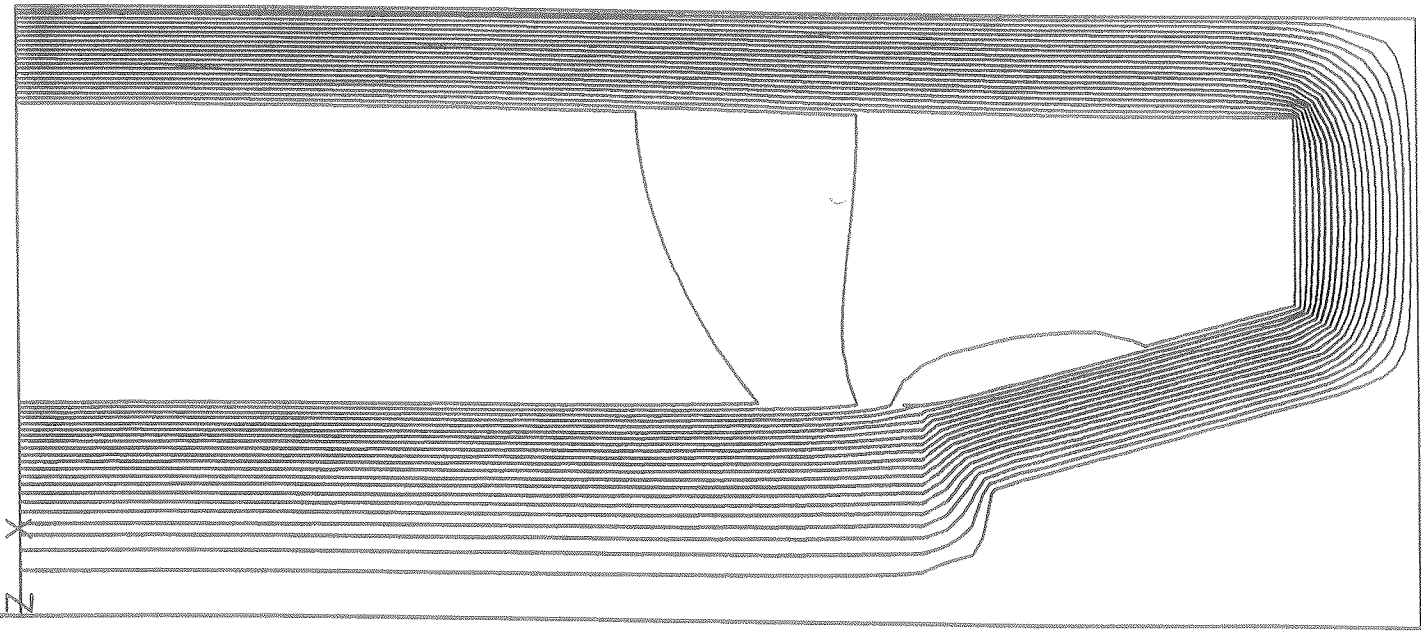


Figure 3. Flux Plot for Iron Return Solenoid

ANSYS 4.4  
DEC 15 1989  
10:00:38  
PLOT NO. 1  
POST1 STRESS  
STEP=2  
ITER=10  
MAG  
SMX =3.301

ZV =1  
\*DIST=4.675  
\*XF =3  
\*YF =-4.25  
EDGE

Flux, Gauss

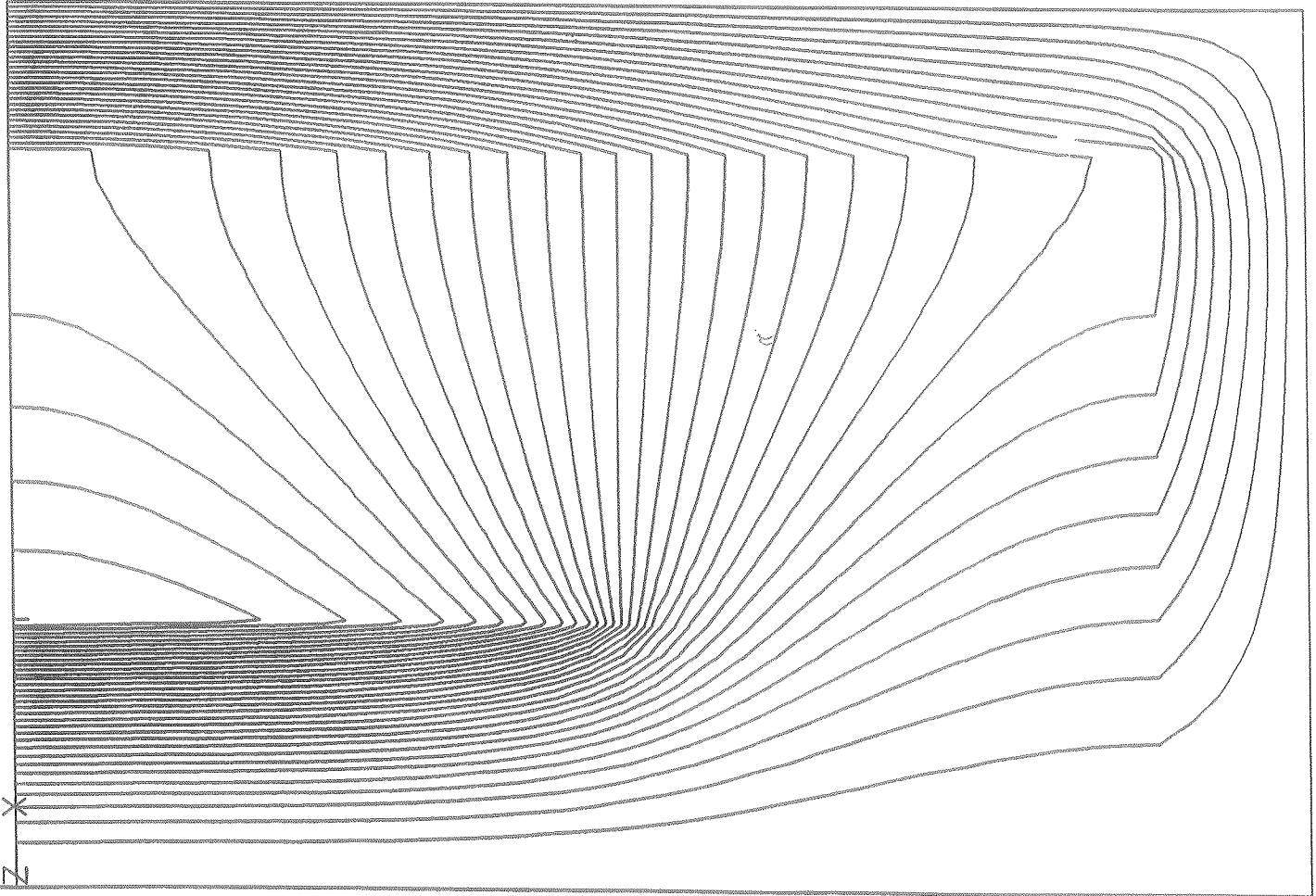


Figure 4. Flux Plot for Air Core Solenoid

# BDL versus Pseudorapidity

Iron Return Solenoid,  $r=1.8$ ,  $BZ=2.0$

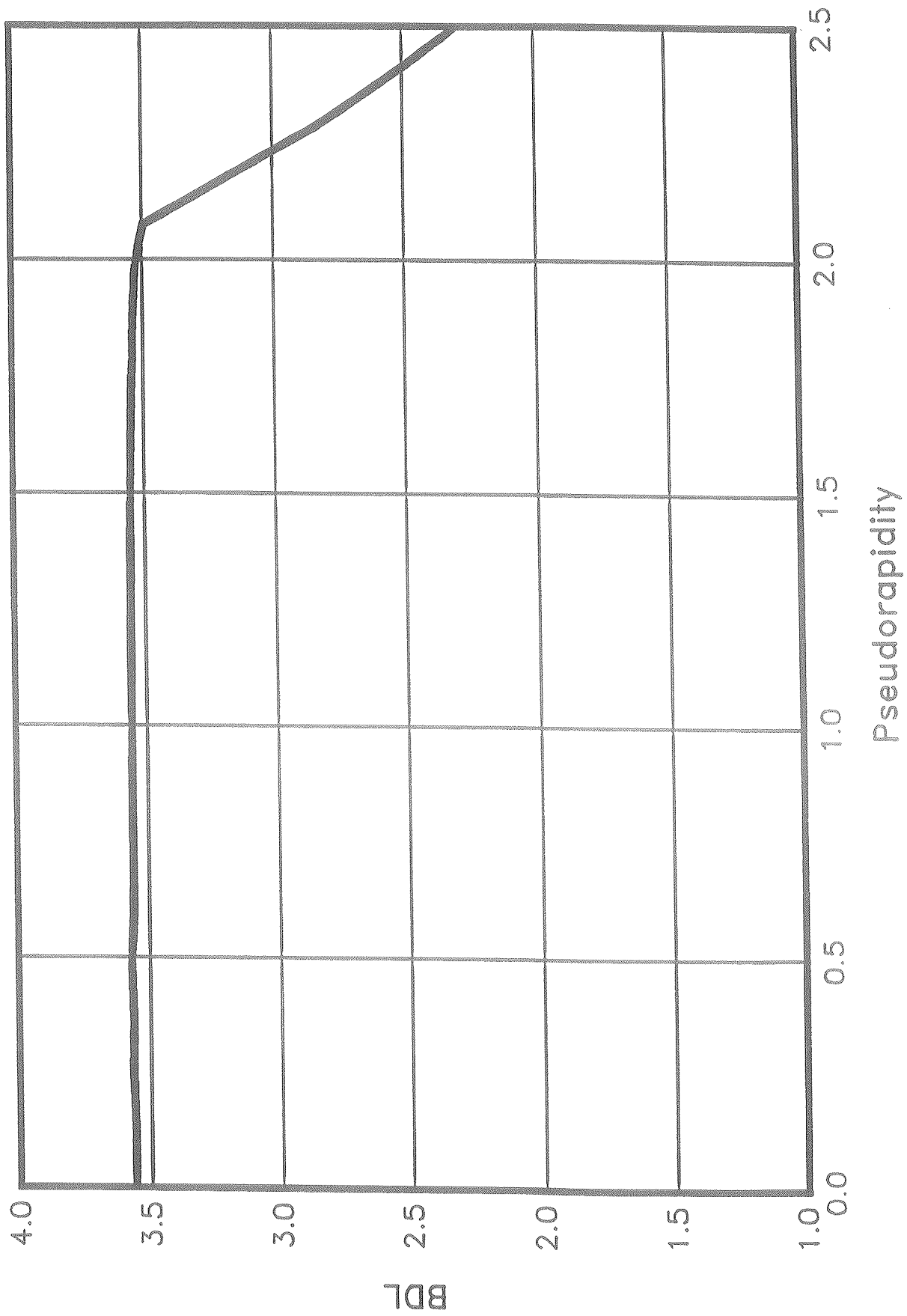
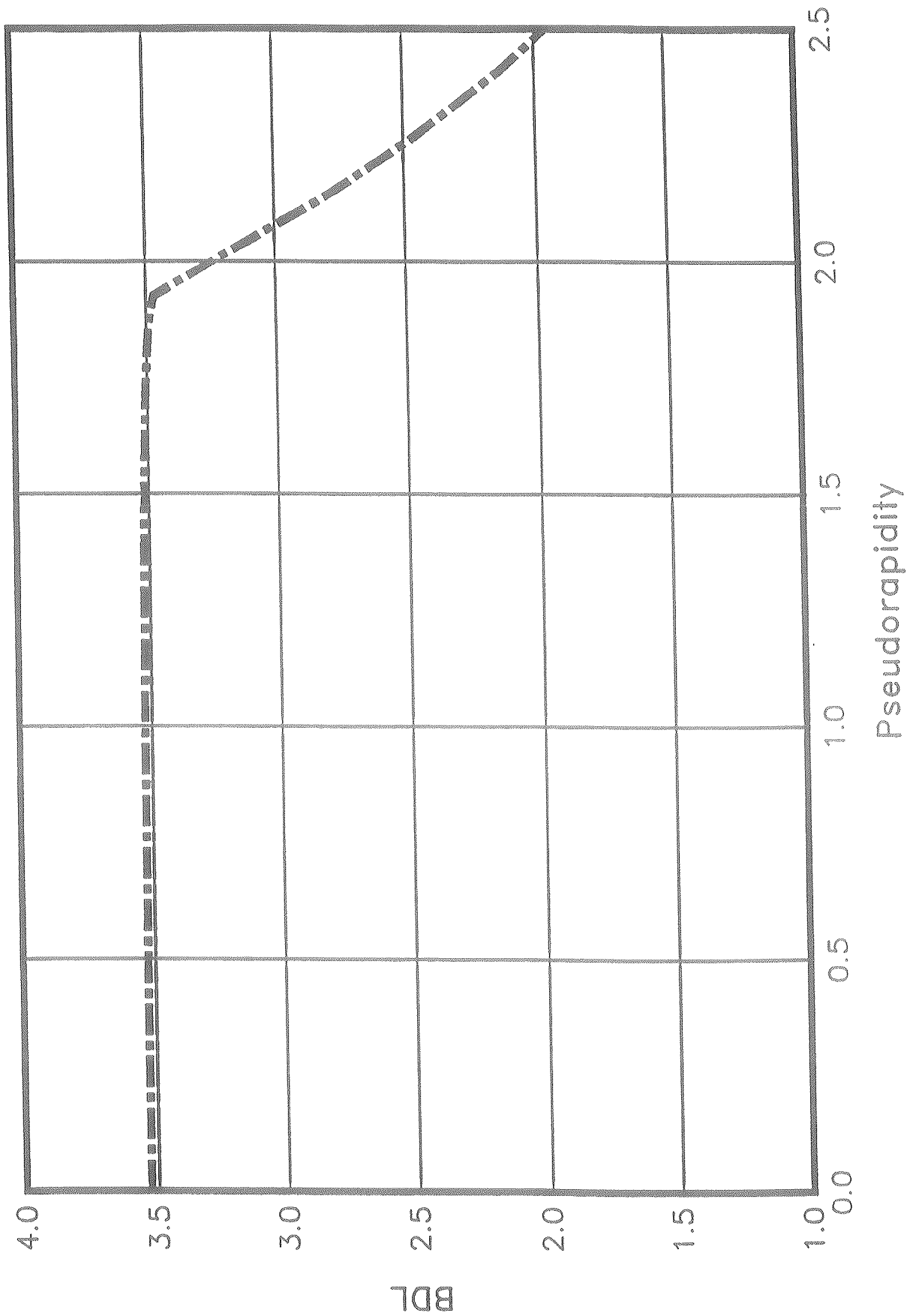


Figure 6.

# BDL versus Pseudorapidity

Iron Return Solenoid,  $r=2.1$ ,  $BZ=1.8$



# BDL versus Pseudorapidity

Air Core Solenoid,  $r=1.8$ ,  $BZ=2.0$

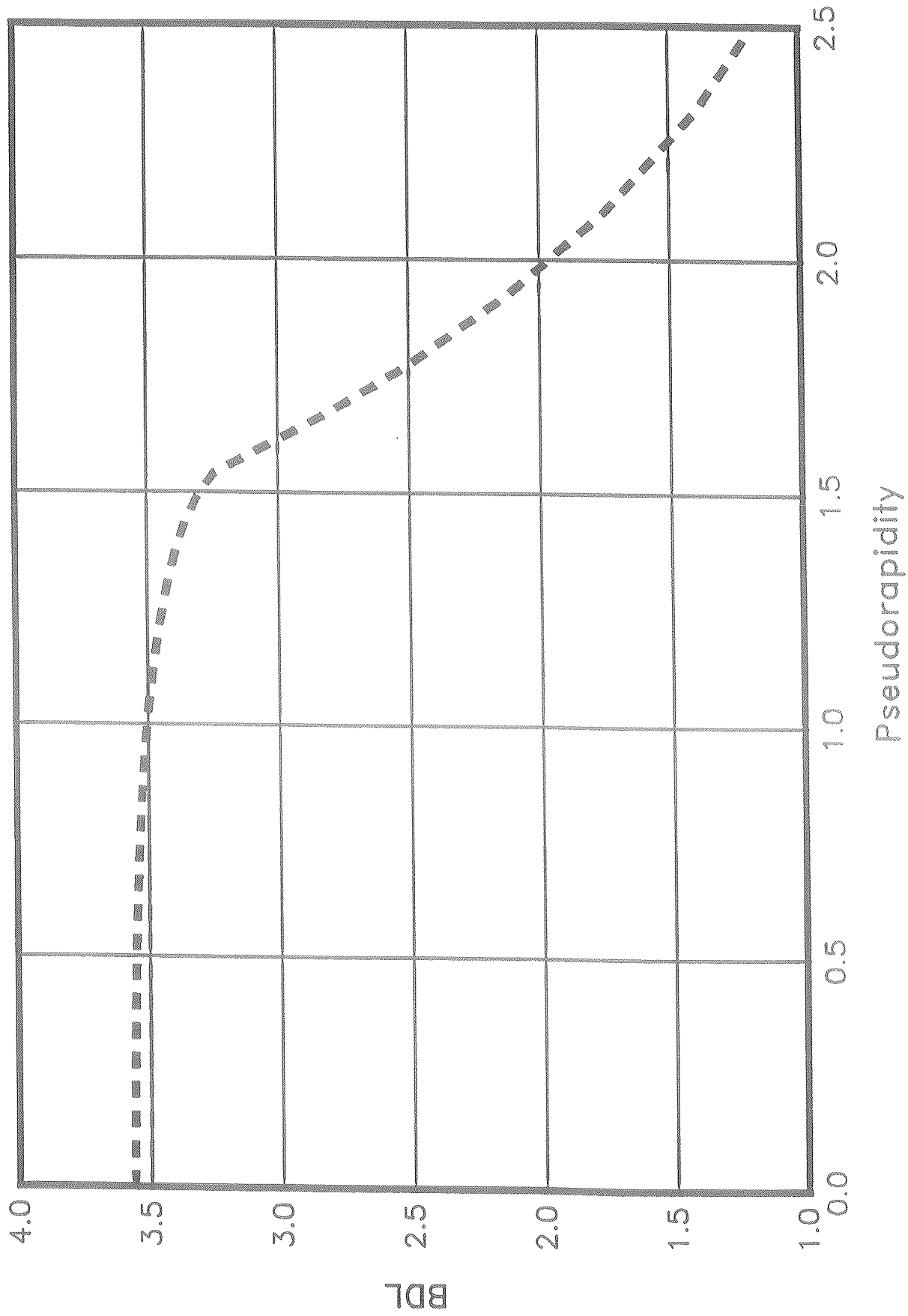


Figure 7.

Figure 8.

# BDL versus Pseudorapidity

Air Core Solenoid,  $r=2.1$ ,  $BZ=1.8$

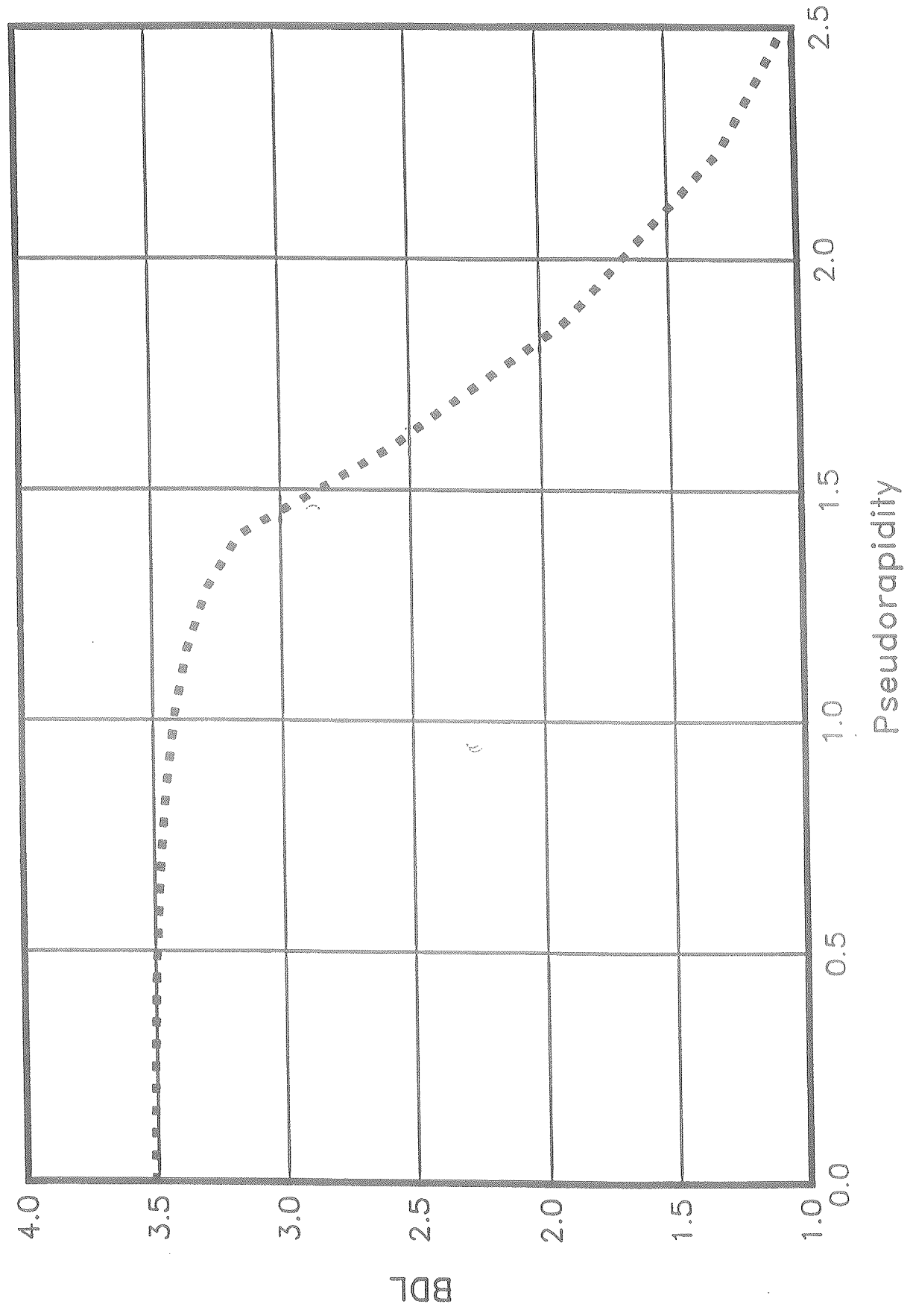


Figure 9.

# BZ versus Pseudorapidity at $r=1.5$ m

Iron Return Solenoid,  $r=1.8$ ,  $BZ=2.0$

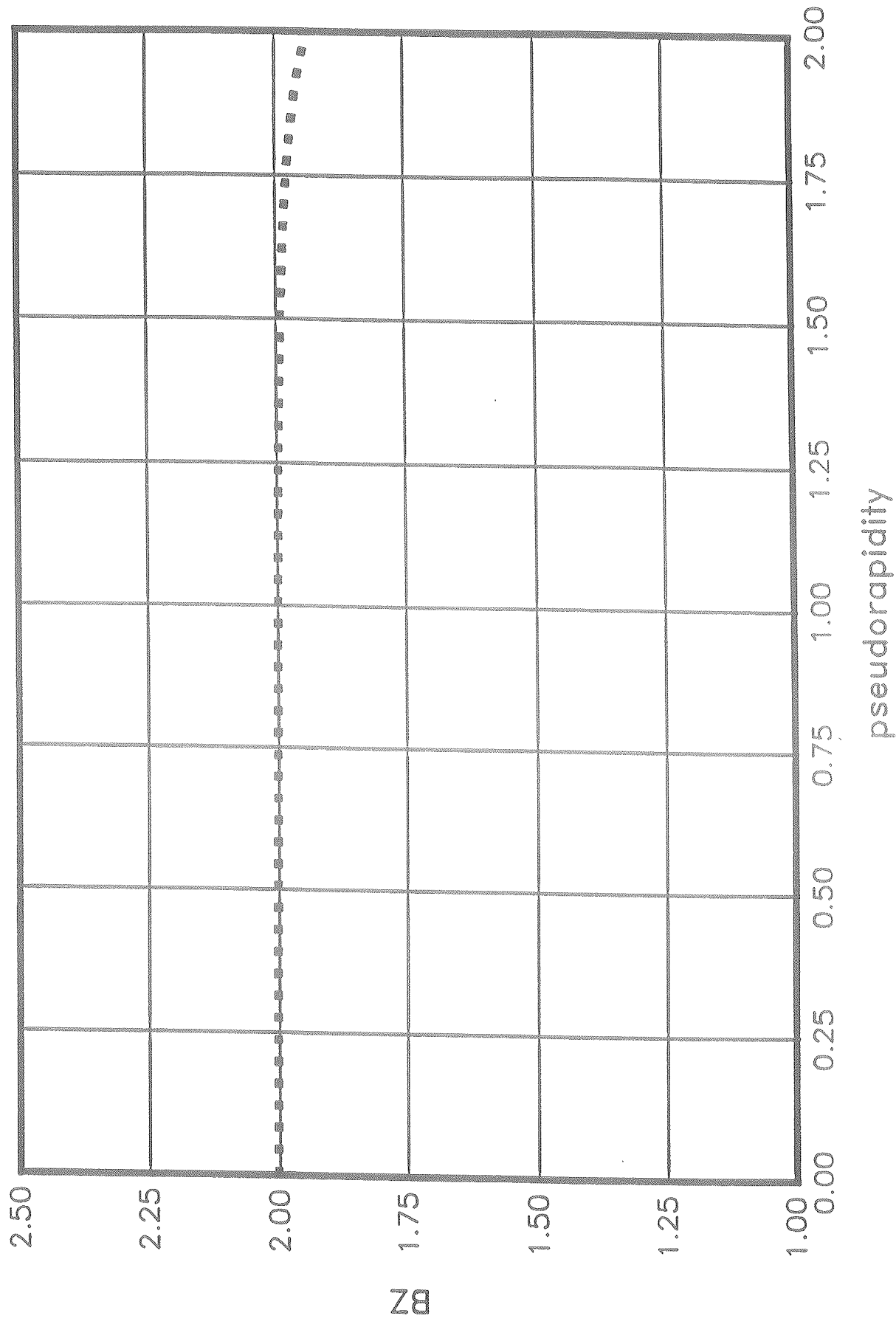
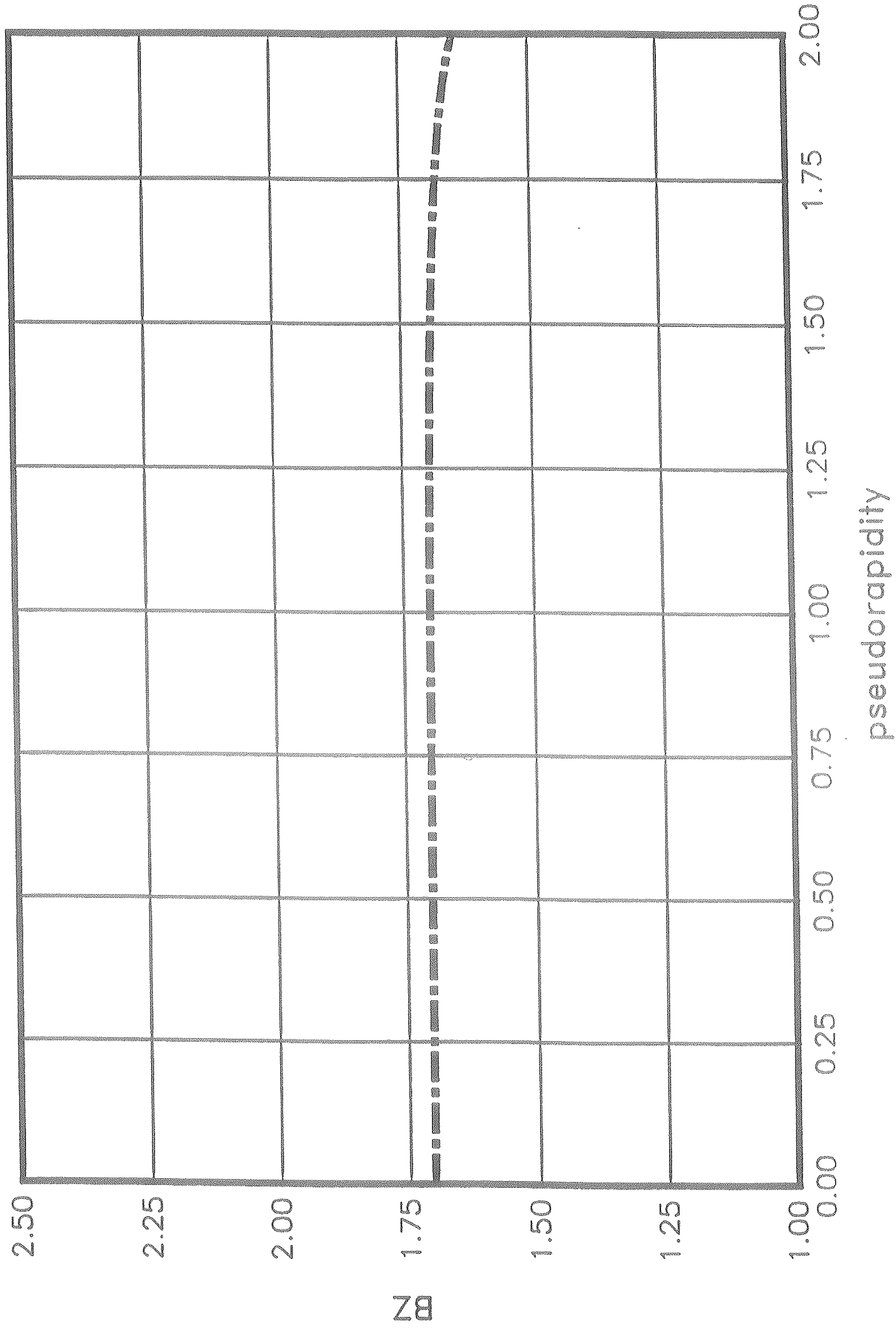


Figure 10.

# BZ versus Pseudorapidity at $r=1.5$ m

Iron Return Solenoid,  $r=2.0$ ,  $BZ=1.8$



# BZ versus Pseudorapidity at $r=1.5$ m

Air Core Solenoid,  $r=1.8$ ,  $BZ=2.0$

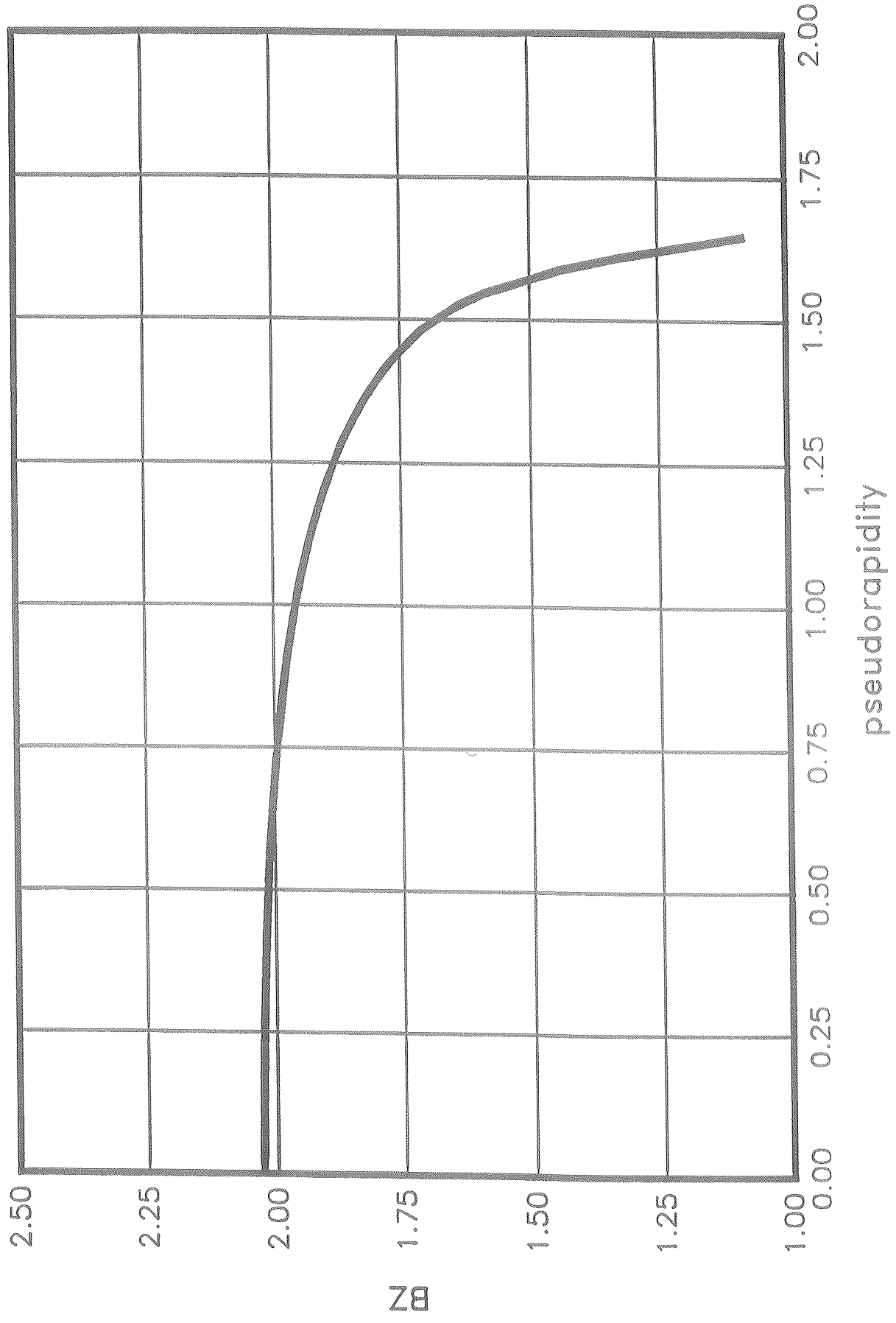
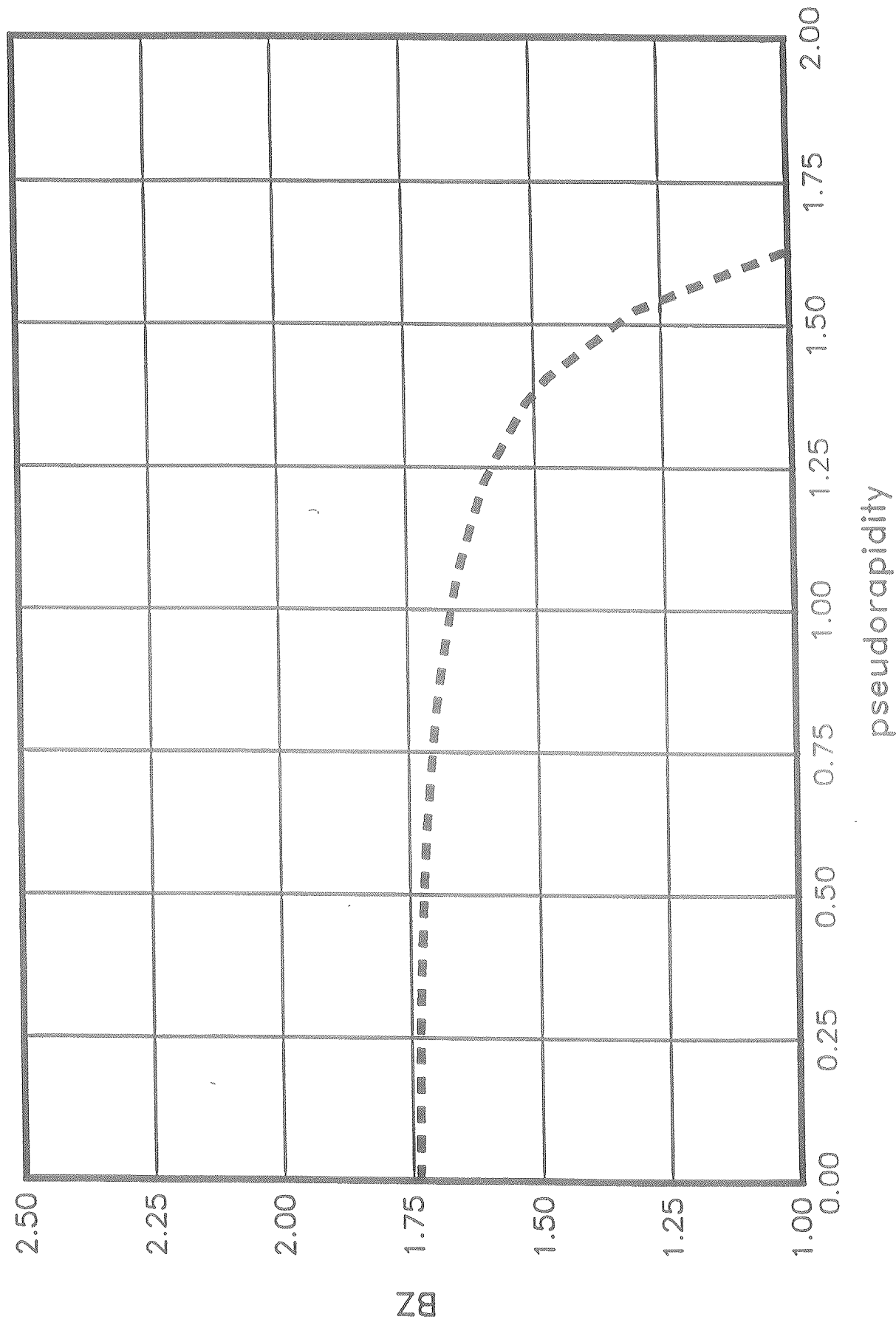


Figure 11.

Figure 12.

# BZ versus Pseudorapidity at $r=1.5$ m

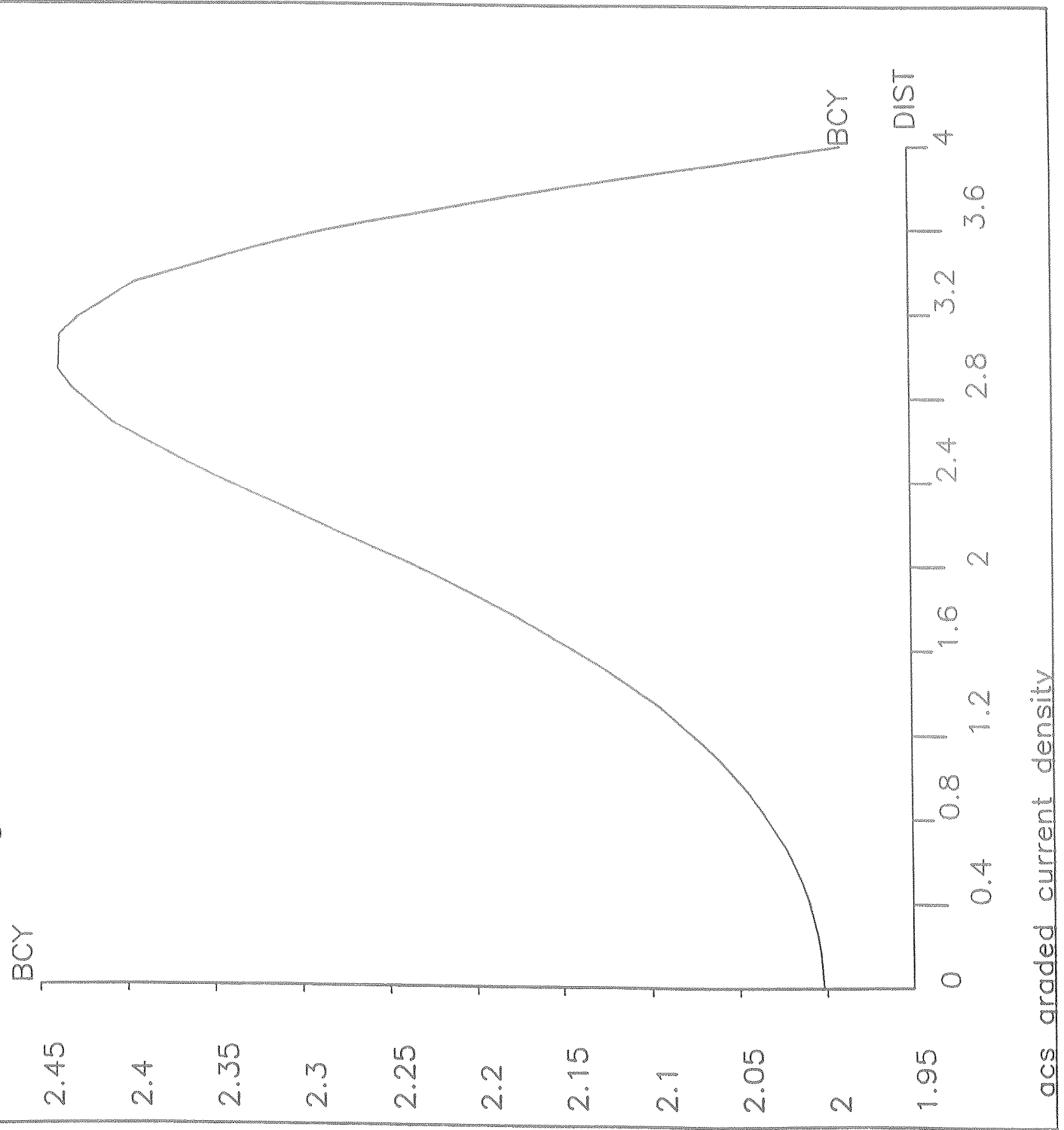
Air Core Solenoid,  $r=2.0$ ,  $BZ=1.8$



ANSYS 4.4  
DEC 18 1989  
15:17:58  
PLOT NO. 1  
POST1  
STEP=2  
ITER=10  
PATH PLOT  
NOD1=569  
NOD2=407  
BCY

ZV =1  
DIST=0.6666  
XF =0.5  
YF =0.5  
ZF =0.5

Figure 13. Axial B-field for ACS-C, Two Current Densities

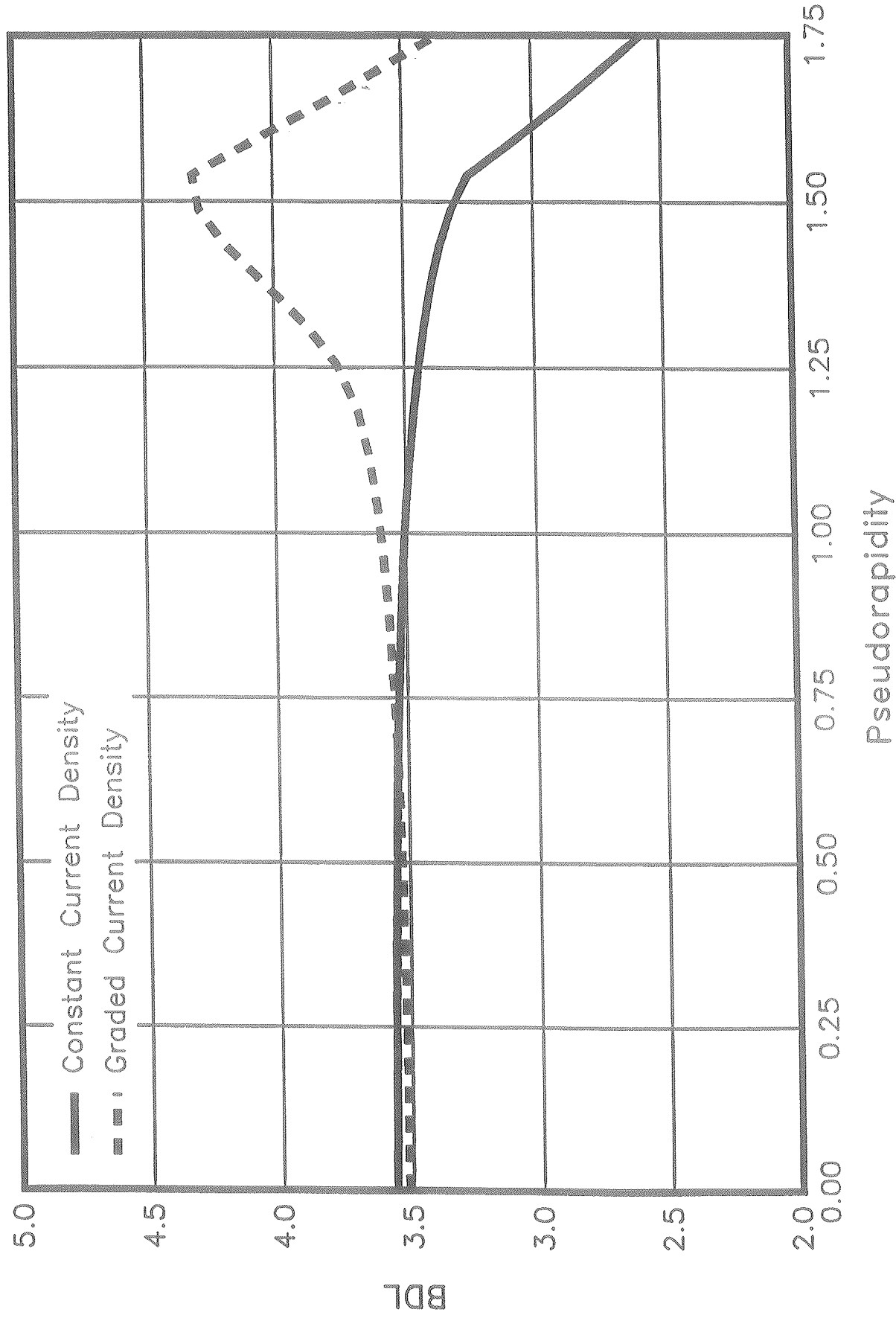


acs graded current density

Figure 14.

# BDL versus Pseudorapidity

Comparison of ACS w/Constant and Graded Cur. Dens.

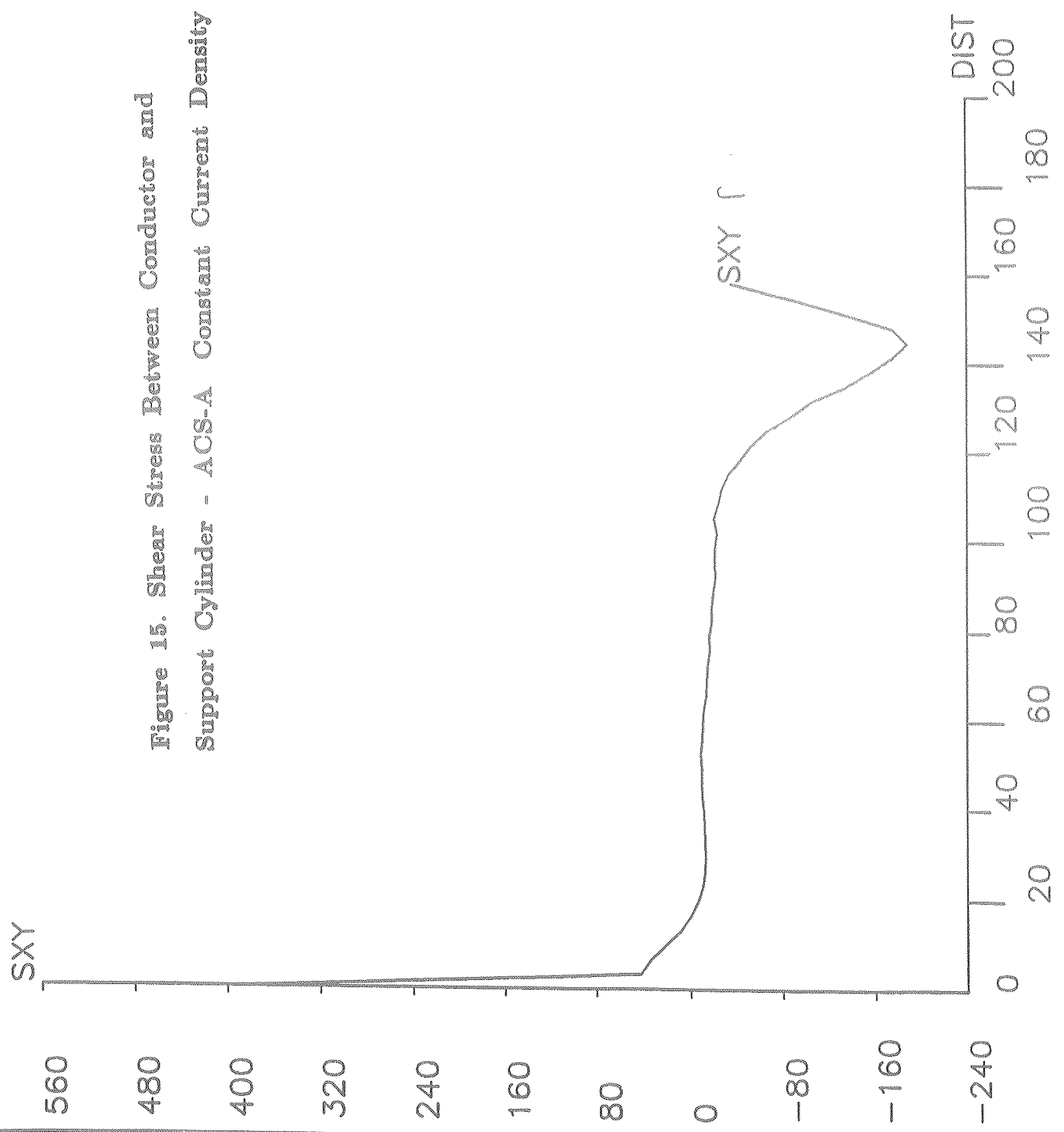


```

ANSYS  4.4
DEC 15 1989
11:22:24
PLOT NO.  1
POST1
STEP=1
ITER=1
PATH PLOT
NOD1=2
NOD2=4
SXY
STRESS GLOBAL
ZV  =1
DIST=0.6666
XF  =0.5
YF  =0.5
ZF  =0.5

```

Figure 15. Shear Stress Between Conductor and Support Cylinder - ACS-A Constant Current Density

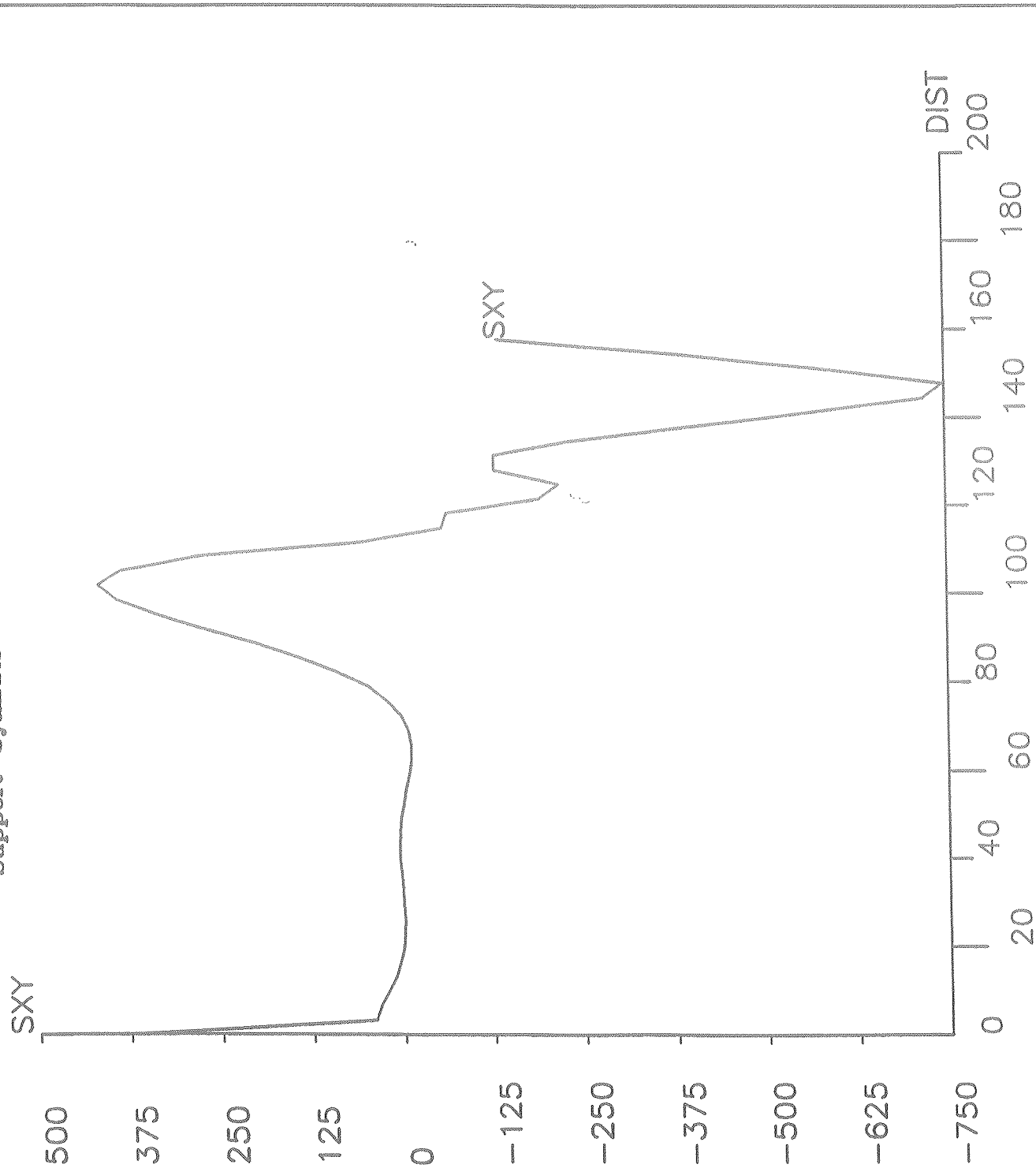


acs const. cur., shear stress at cylinder

ANSYS 4.4  
 DEC 15 1989  
 11:23:08  
 PLOT NO. 2  
 POST1  
 STEP=2  
 ITER=1  
 PATH PLOT  
 NOD1=2  
 NOD2=4  
 SXY  
 STRESS GLOBAL

ZV =1  
 DIST=0.6666  
 XF =0.5  
 YF =0.5  
 ZF =0.5

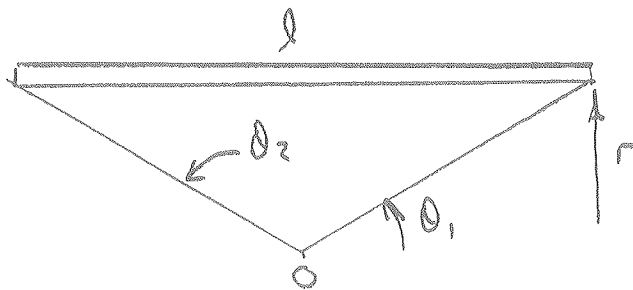
Figure 16. Shear Stress Between Conductor and Support Cylinder - ACS-C Two Current Densities



acs graded cur. dens. shear stress at cylinder

Appendix A  
 Calculation of Current Densities for ACS  
 w/ Two Current Densities

For a uniform current density  $I_0$ , and  $n_0$  turns/length of solenoid

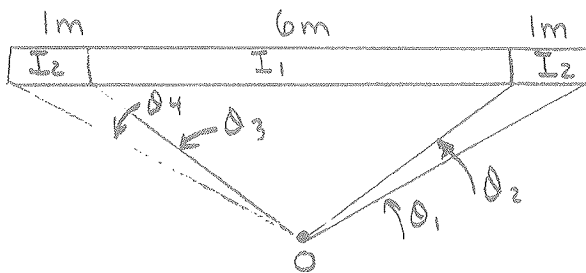


$$B_z @ O = \frac{1}{2} \mu n_0 I_0 (\cos \theta_2 - \cos \theta_1)$$

For the ACS, with  $\frac{1}{2} \mu n = k$ ,  $\theta_1 = 24.22$ ,  $\theta_2 = 155.77$ ,  $r = 1.8$ ,  $l = 8m$

$$B_z = -1.82388 k n_0 I_0$$

For two current densities



$$\theta_1 = 24.22$$

$$\theta_2 = 30.96$$

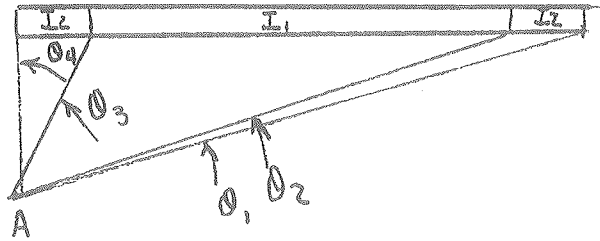
$$\theta_3 = 149.036$$

$$\theta_4 = 155.77$$

$$B_z = k n_2 I_2 (2)(-0.0544) + k n_1 I_1 (-1.7150)$$

$$B_z = -1.7150 k n_1 I_1 - 0.1088 k n_2 I_2$$

(2)



$$\theta_1 = 12.68$$

$$\theta_2 = 14.42$$

$$\theta_3 = 60.94$$

$$\theta_4 = 90.0$$

$$B_z = \mu_0 \mu_1 I_2 \left[ (-0.00711) + (-0.48572) \right] + \mu_0 \mu_1 I_1 (-0.4827)$$

$$B_z = -0.4827 \mu_0 \mu_1 I_1 - 0.49283 \mu_0 \mu_1 I_2$$

If  $B_z$  w/2 currents =  $B_z$  uniform

$$(1) \quad -0.4827 \frac{\mu_0 \mu_1 I_1}{\mu_0 I_0} - 0.49283 \frac{\mu_0 \mu_1 I_2}{\mu_0 I_0} = -1.82388$$

$$(2) \quad -1.7150 \frac{\mu_0 \mu_1 I_1}{\mu_0 I_0} - 0.1088 \frac{\mu_0 \mu_1 I_2}{\mu_0 I_0} = -1.82388$$

Solving,

$$1.7150 C_1 + 1.75099 C_2 = 6.48012$$

$$1.7150 C_1 + 0.1088 C_2 = 1.82388$$

$$1.64219 C_2 = 4.65624$$

$$C_2 = 2.83$$

$$C_1 = 0.889$$

Therefore,

$$\frac{n_1 I_1}{n_0 I_0} = 0.889$$

$$\frac{n_2 I_2}{n_0 I_0} = 2.83$$

If the ANSYS uniform current density is  $CD_0$ , and the thickness of the conductor elements is constant along the length of the solenoid

$$CD = 0.889 CD_0$$

$$CD_1 = 2.83 CD_0$$